

RESEARCH

Open Access



circ_0002970 promotes fibroblast-like synoviocytes invasion and the inflammatory response through Hippo/YAP signaling to induce CTGF/CCN1 expression in rheumatoid arthritis

Haoran Kong^{1†}, Yushuang Qiao^{1†}, Dahu Qi^{1†}, Shixin Zhao¹, Zhiming Cao¹, Junhao Feng¹, Yitong Li¹, Yunke Liu^{1*} and Tao Liu^{1*}

Abstract

Background Rheumatoid arthritis (RA) is a chronic autoimmune disorder characterized by synovial inflammation, hyperplasia, and joint destruction. Fibroblast-like synoviocytes (FLSs) are key effector cells in RA, contributing to synovial invasion, extracellular matrix degradation, and inflammatory cytokine secretion. Recent studies suggest that circular RNAs (circRNAs) regulate cellular function and disease progression, but their role in RA remains unclear. The Hippo-YAP signaling pathway governs cell proliferation, apoptosis, and extracellular matrix remodeling, and its dysregulation is linked to RA synovial hyperplasia and inflammation. However, whether circRNAs regulate Hippo-YAP signaling in RA-FLSs has not been fully elucidated. This study investigates the role of circ_0002970 in RA progression and its regulation of the Hippo-YAP pathway.

Methods Synovial tissues from RA patients, osteoarthritis (OA) patients, and healthy controls were collected. Differentially expressed circRNAs were identified via RNA sequencing. The expression of circ_0002970 was validated via qRT-PCR, FISH, and RNase R digestion assays. The functional experiments included transfection, migration/invasion assays, ELISA, and Western blotting to evaluate its role in RA-FLSs.

Results Circ_0002970 was significantly upregulated in RA-FLSs. Knockdown of circ_0002970 suppressed RA-FLS migration, invasion, and IL-6 secretion. Mechanistically, circ_0002970 knockdown downregulated the expression of Hippo-YAP pathway components (YAP, CTGF, and CCN1) and decreased the expression of MMP-9 and MMP-13, which

[†]Haoran Kong, Yushuang Qiao and Dahu Qi contributed equally to this work.

*Correspondence:

Yunke Liu
liuyunke@zzu.edu
Tao Liu
liutaogk@163.com

Full list of author information is available at the end of the article



are critical for cartilage degradation. Furthermore, verteporfin (VP)-mediated inhibition of Hippo-YAP reversed the effects of circ_0002970 overexpression.

Conclusion These findings highlight circ_0002970 as a novel regulator of RA-FLS migration, invasion, and inflammation via the Hippo-YAP signaling pathway.

Introduction

Rheumatoid arthritis (RA) is a common chronic autoimmune disease characterized by synovial inflammation and joint damage [1, 2]. In recent decades, significant advances in the treatment of RA have improved outcomes [3, 4]. However, a subset of patients are still affected by persistent inflammation and progressive disability [5, 6]. The underlying pathophysiological mechanisms of RA still require further exploration.

Previous studies have shown that some stromal cells, particularly fibroblast-like synovial RA-FLSs, have invasive properties that are not observed in other fibroblasts [7, 8]. In addition, RA-FLSs are considered the primary effectors of cartilage destruction through the secretion of proteases, especially matrix metalloproteinases (MMPs) and cathepsins [9–11]. Some inflammatory factors, such as TNF- α and IL-1 β , secreted by macrophages can also enhance the destructive properties of RA-FLSs [12, 13]. Additionally, activated RA-FLSs further strengthen the inflammatory cycle and maintain the inflammatory environment persistently by establishing paracrine/autocrine networks [14, 15]. In vivo animal studies have shown that RA-FLSs can maintain their invasive phenotype in the absence of interference from other cells [16]. Therefore, the concept of targeting FLSs has great potential for the treatment of RA. Thus, further exploration of the internal mechanism is urgently needed to identify new and more effective treatment methods.

Circular RNAs (circRNAs) are particularly stable RNAs in vivo that are generated from protein-coding genes via the spliceosome by backsplicing [17, 18]. Among these, circRNAs are found mainly in the cytoplasm of eukaryotic cells, and their expression is usually irrelevant to that of the host gene [19]. CircRNAs show great potential in regulating molecular expression through several mechanisms, including alternative splicing, miRNA sponging and RNA binding protein interactions [20–22]. Few studies have shown that circRNAs are found in most joint tissues and play crucial roles in the pathogenesis and development of RA. For example, Cai reported that circ_0088194 promotes the invasion and migration of RA-FLSs via the miR-766-3p/MMP2 axis [23]. However, the expression data and functions of only a few circRNAs have been elucidated. Through sequencing analysis, we identified that circ_0002970 is abnormally upregulated in RA-FLSs. Knockdown of circ_0002970 led to a decrease in RA-FLS migration and invasion abilities. Moreover, as no prior studies have investigated the function

and underlying mechanisms of circ_0002970 in RA, we selected it as the research target for this study.

The Hippo signaling pathway, initially discovered in *Drosophila*, is well known for its role in regulating organ size and tissue growth and is considered a highly conserved signaling cascade [24]. Previous studies have reported that the key effector protein YAP in the Hippo signaling pathway is upregulated in RA-FLSs. Conversely, YAP downregulation has been shown to inhibit FLS migration and invasion, thereby mitigating the severity of arthritis [25].

In this study, we identified a novel circRNA, circ_0002970, in RA-FLSs, which regulates the Hippo-YAP pathway and subsequently affects the expression of CCN1 and CTGF. Through this mechanism, circ_0002970 modulates RA-FLS migration, invasion, and the release of inflammatory factors.

Materials and methods

Patients and specimens

The diagnostic criteria for patients with RA were based on the American College of Rheumatology criteria [26]. The diagnostic criteria for patients with OA were based on the classification criteria from the ARC in 1986. Synovial tissues from patients with OA or RA who underwent total knee replacement were obtained. Normal synovial tissues were obtained from young patients with meniscus injury or cruciate ligament injury who underwent arthroscopic surgery. Ethical approval was obtained from the Ethics Committee of Henan Provincial People's Hospital (Zhengzhou, China, LLXJS2023-1-137). A total of 12 RA patients (7 females, 5 males; mean age 56.8 ± 4.1 years), 11 OA patients (6 females, 5 males; mean age 55.0 ± 6.1 years), and 7 healthy controls (3 females, 4 males; mean age 26.7 ± 2.2 years) were enrolled in the study. The disease duration was 8.5 ± 3.2 years for RA patients and 10.2 ± 4.1 years for OA patients. Written informed consent was obtained from all participants.

Cell isolation and culture

The synovial tissues from patients were washed with PBS under sterile conditions. Then, fat tissues were carefully removed with ophthalmic scissors, and the tissues were cut into small pieces. The tissues were digested with 2.5% type I collagenase (Biosharp, Hefei, China) for 2 h in a constant-temperature shaker. Single-cell suspensions were subsequently prepared through a cell strainer. The cells were cultured in DMEM (Gibco) supplemented

with 10% fetal bovine serum (Hangzhou Sijiqing, China) and incubated at 37 °C with 5% CO₂. The cells were used after passages 3–5 for subsequent experiments.

Identification of differentially expressed circrnas

FLSs were isolated from three healthy controls, three OA patients, and three RA patients. The total RNA of FLSs was collected for circRNA sequencing. The circRNA library was constructed via rRNA removal and linear RNA digestion. Purified and enriched circRNAs were fragmented and used for cDNA synthesis to construct the library. The purified double-stranded cDNA was subsequently subjected to end-repair, dA-tailing and adaptor ligation. The cDNA products were circularized and amplified via PCR and subsequently used for DNB generation. Finally, each DNB was loaded into a lane for subsequent sequencing on a BGISEQ-500 platform (MGI, Shenzhen, China). The circRNA candidates were detected by using `find_circ`, as abnormal fragments were discarded [21]. CircRNAs with $|log(\text{fold change})| > 2$ and adjusted P value < 0.05 were set as the significant cutoffs. Gene Ontology (GO) analysis and enrichment analysis of these differentially expressed circRNAs were performed via Sanger box 3.0.

RNase R treatment

To assess the stability of circRNAs, linear mRNA was digested with RNase R (Beyotime). The RNase R treatment was performed in a 20 µL reaction system, which included ≤ 5 µg of total RNA, 2 µL of 10X RNase R Reaction Buffer, and RNase R (20 U/µL) at a final concentration of 1–3 U per µg of RNA. The reaction volume was adjusted to 20 µL using DEPC-treated water. The mixture was then incubated at 37 °C for 30 min to allow complete digestion of linear RNA. After treatment, the stability of the circRNAs was determined by qRT-PCR.

Sanger sequencing

Further verification of the accuracy of circRNA primer amplification was performed via Sanger sequencing by Company. (Shenzhen, China)

Nucleic acid transfections

RA-FLSs were grown in 12-well plates and reached 60–80% confluence for subsequent transfection. siRNAs against `hsa_circ_0002970` and negative control siRNA were purchased from Genesee Technology (China). The target sequences for siRNA-mediated knockdown of `circ_0002970` were as follows: (1) Si-`hsa_circ_0002970-1`: CAATGGCTTGTTGGGAAAC(dT)(dT); (2) Si-`hsa_circ_0002970-2`: AATGGCTTGTTGGGAAACC(dT)(dT); (3) Si-`hsa_circ_0002970-3`: ATGGCTTGTTGGGAAACCA(dT)(dT); (4) Si-NC: UUCUCCGAACGUGUCACGUTT(dT)(dT). The negative control siRNA that

was labeled with FAM was used to visualize the uptake of the siRNA. The transfection was performed by using Lipofectamine® RNAiMAX Reagent (Thermo Fisher Scientific). Opti-MEM reduced serum medium was used to dilute the siRNAs, and Lipofectamine® RNAiMAX Reagent was used.

Lentiviral transfection

Lentiviral vectors for `circ_0002970` overexpression (LV-`circ_0002970`) and negative control (LV-NC) were designed and synthesized by HANBIO (Shanghai, China). RA-FLSs were seeded in six-well plates and cultured until they reached 50–70% confluence. The cells were then infected with lentivirus at an appropriate multiplicity of infection (MOI) in the presence of 5 µg/mL polybrene to enhance transduction efficiency. After 24 h, the medium was replaced with fresh complete DMEM, and cells were further cultured for 48–72 h. For stable expression, cells were selected using 2 µg/mL puromycin for 5–7 days.

ELISA kit

An IL-6 human ELISA kit (Ruixin Biotech, QuanZhou, China) was used. RA-FLSs were plated on 6-well plates. After `circ_0002970` was knocked down, the cells were incubated with DMEM containing 10% fetal bovine serum for 24 h. The supernatant was collected to measure the IL-6 levels.

Migration and invasion assays

The migration and invasion abilities of FLSs were assessed using 24-well Transwell chambers with 8 µm pore-size polycarbonate membranes (Corning). For the invasion assay, Matrigel was pre-diluted on ice at a ratio of 8:1 (FBS: Matrigel) and evenly coated onto the upper surface of the Transwell insert. The coated chambers were incubated at 37 °C for 4–5 h to allow polymerization. For the migration assay, no Matrigel coating was applied. After Matrigel polymerization, 200 µL of a serum-free DMEM cell suspension containing FLSs was added to the upper chamber, while 600 µL of DMEM supplemented with 5% FBS was added to the lower chamber to create a chemoattractant gradient. The cells were incubated at 37 °C in a humidified incubator with 5% CO₂ for 24 h to allow migration (or invasion). Following incubation, the non-migrated or non-invaded cells on the upper surface of the membrane were gently removed using a cotton swab. The membranes were then fixed with 4% paraformaldehyde for 15 min and stained with crystal violet solution for 15 min. The stained cells were visualized using an inverted microscope, and the number of migrated or invaded cells was counted in four randomly selected fields ($\times 200$ magnification).

RNA labeling and fluorescence in situ hybridization

FISH analysis of RA-FLSs was performed using biotin-labeled probes specific to circ_0002970 (Servicebio, Wuhan, China). RA-FLSs were cultured on glass coverslips and then fixed with 4% paraformaldehyde. The cells were permeabilized with 0.1% Triton X-100, followed by prehybridization at 37 °C. Biotin-labeled probes specific to circ_0002970 were hybridized overnight at 37 °C. After posthybridization washes with 2x and 0.5x SSC buffer, the probes were detected via a fluorescently labeled streptavidin conjugate. Nuclei were counterstained with DAPI, and the coverslips were mounted on slides with antifade medium. Finally, cell observation and fluorescence imaging were performed via a fluorescence microscope (Nikon, Tokyo, Japan).

Agarose gel electrophoresis

The qPCR products amplified by convergent primers and divergent primers were subjected to 1.5% agarose gel electrophoresis. First, the agarose was diluted with Tris-acetate-EDTA buffer in a erlenmeyer flask and then heated in a micro-wave oven. Then, the cDNA and gDNA qPCR products were mixed with loading buffer added to the agarose gel well, a suitable ladder was chosen and separated at 110 V for 30 min. The gel was soaked in ethidium bromide to stain the DNA fragments and visualized in an automatic gel imaging system (DYY-8c, Beijing Liuyi Co., Ltd., Beijing, China).

Quantitative real-time PCR validation

The total RNA of FLSs was extracted via the FastPure Cell/Tissue Total RNA Isolation Kit (RC112, Vazyme Biotech). The gDNA of FLS was extracted via the FastPure® Cell/Tissue DNA Isolation Mini Kit (DC102, Vazyme Biotech). Then, qRT-PCR was performed via a ChamQ Universal SYBR qPCR Master Mix Kit (Q711, Vazyme Biotech) in a 7500 Fast Real-time quantitative PCR system according to the standard procedure (Thermo Fisher Scientific). The relative gene expression of the circRNAs and mRNAs was analyzed via normalization to the expression of GAPDH via the $2^{-\Delta\Delta Ct}$ method. The linear and circular RNA primers used in this study were synthesized by Shangya Biotechnology Co., Ltd. (Supplementary material 1).

HE staining

The synovial tissues were excised from the knee joints, fixed in 10% neutral formalin, decalcified in EDTA, embedded in paraffin, sectioned, and stained with hematoxylin-eosin (HE).

Western blotting

FLSs were grown in 6-well plates and treated differently (2×10^5 /well). Then, the cells were lysed in a mixture of

RIPA lysis buffer (Thermo Fisher Scientific) with 1 tablet of protease inhibitor and 1 tablet of phosphatase inhibitor (MedChemExpress) for protein extraction. A BCA protein assay kit (Beyotime, China) was used for protein concentration determination and standardized quantification. SDS-PAGE was used to resolve the proteins, which were then transferred to PVDF membranes. Western blotting was carried out according to standard procedures. The membranes were incubated with specific antibodies and then visualized via ChemiDoc XRS (Bio-Rad). To ensure reproducibility, WB experiments were performed with biological triplicates ($n=3$ per group, each representing an independent sample).

Statistical analysis

All the experiments were repeated at least three times. GraphPad Prism 9 and SPSS 26.0 software were used for statistical analysis. All the data are presented as the means \pm standard deviations. Differences between two groups were analyzed via Student's t test, whereas differences among three or more groups were analyzed via one-way ANOVA. $P < 0.05$ was considered statistically significant.

Results

Comparative analysis of synovial histological features and differential gene expression

First, synovial tissues were divided into three groups (CON group = 7, OA group = 11, RA group = 12) and subjected to H&E staining and X-ray analysis. As shown in Fig. 1A, the RA group exhibited severe synovial hyperplasia and inflammation compared with the other two groups according to H&E staining. X-ray analysis revealed more pronounced joint space narrowing and periarticular osteopenia in the RA group. CircRNA transcriptome sequencing was performed on FLSs isolated from three RA patients, three OA patients, and three healthy controls. The differentially expressed genes (DEGs) among the groups are illustrated in a box plot (Fig. 1B). Heatmaps and scatter plots were then used to compare the DEGs between the two sample groups (Fig. 1C-E). Differential analysis revealed that several circRNA genes were upregulated or downregulated in the RA samples compared with those in the OA and control samples. The number of upregulated and downregulated DEGs between the two sample groups was quantified via bar charts (Fig. 1F). Finally, the intersection of DEGs between the CON vs. RA and OA vs. RA comparisons was depicted via Venn diagrams (Fig. 1G), suggesting that these genes might participate in the migration and invasion of RA-FLSs.

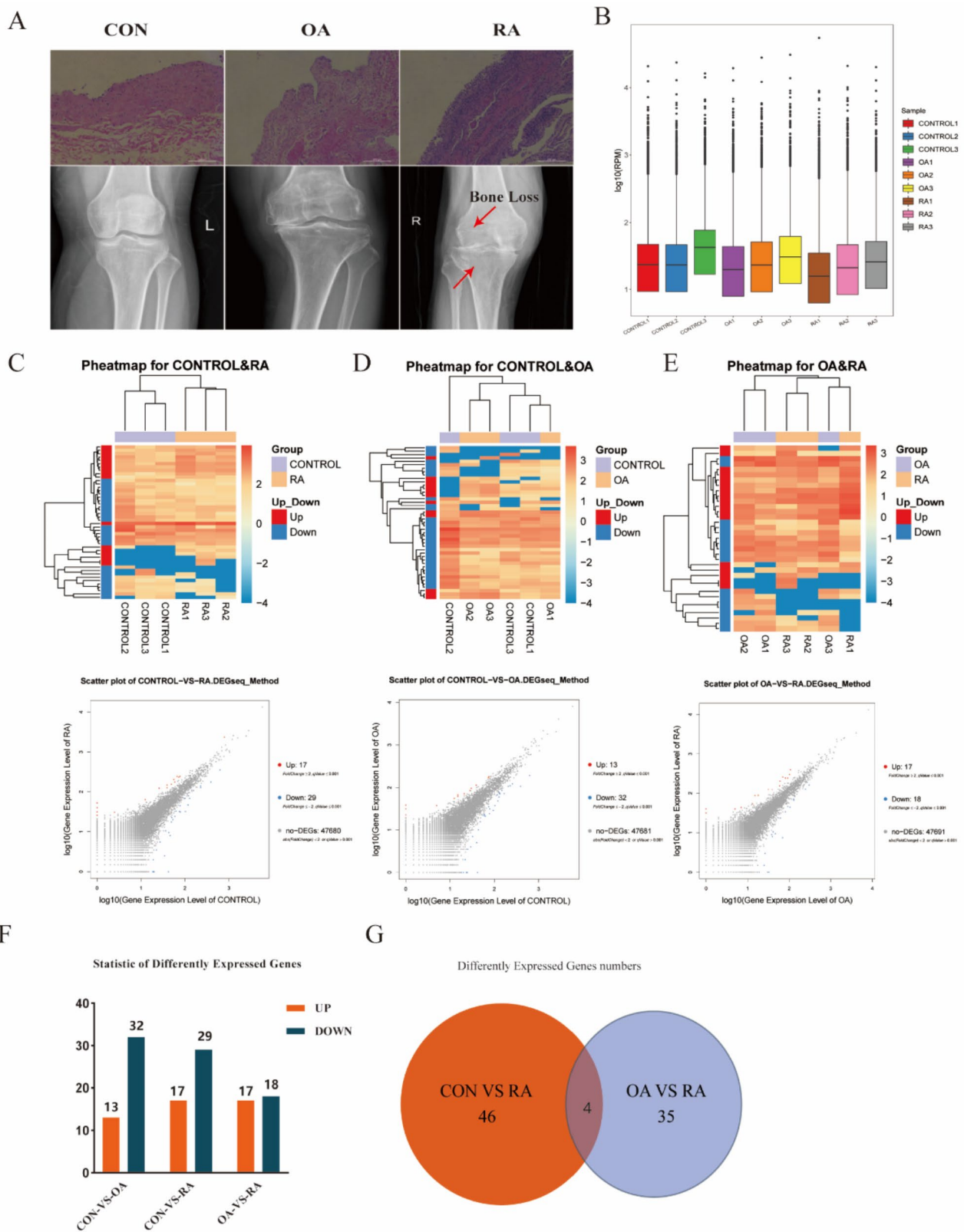


Fig. 1 (See legend on next page.)

(See figure on previous page.)

Fig. 1 Histological, radiological, and transcriptomic analysis of the three groups of synovial tissues. **(A)** Histology and X-ray images of synovial tissues. H&E staining shows synovial hyperplasia and inflammation in RA compared to OA and control. X-ray images reveal bone loss in RA. **(B)** Gene expression distribution. Box plot showing $\log_{10}(\text{FPKM})$ values across groups. **(C-E)** Differentially expressed genes (DEGs). Heatmaps and scatter plots of DEGs in RA vs. control **(C)**, OA vs. control **(D)**, and RA vs. OA **(E)**. Upregulated genes are in red, downregulated in blue. **(F)** DEG statistics. Bar graph showing the number of upregulated (orange) and downregulated (blue) genes in different comparisons. **(G)** Venn diagram of DEGs. 46 DEGs in CON vs. RA, 35 DEGs in OA vs. RA, with 4 overlapping genes. Scale bar, 200 μm

Functional enrichment analysis of the differentially expressed circrnas

To explore the functional roles of the identified DEGs, we performed GO and KEGG pathway enrichment analyses between the CON and RA groups, as well as between the OA and RA groups. Gene Ontology enrichment analysis revealed that the DEGs were enriched in biological processes (BP), molecular functions (MF) and cellular components (CC), such as cellular processes, cellular anatomical entities, and binding (Fig. 2A-B). In addition, Kyoto Encyclopedia of Genes and Genomes (KEGG) enrichment analysis revealed differentially enriched signaling pathways, such as the IL-17, MAPK, GnRH, and cAMP signaling pathways. (Fig. 2C-D). The GO and KEGG enrichment results suggest that differentially expressed circRNAs may be involved in key RA-related pathways, such as inflammation, extracellular matrix remodeling, and cell migration, potentially contributing to RA-FLS dysfunction.

Expression and characterization of circ_0002970 in RA-FLSs

FLSs were derived from synovial tissues of the three groups, and several significantly different circRNAs were selected for expression analysis via transcriptome sequencing (Fig. 3A). Circ_0002970 exhibits the most significant differences among the three groups, and its host gene, CEMIP, is closely associated with inflammation and extracellular matrix degradation. To confirm circ_0002970, divergent and convergent primers for RT-PCR were designed to amplify circ_0002970 from cDNA but not from gDNA, while the control gene GAPDH was amplified from both cDNA and gDNA, confirming that circ_0002970 is indeed a circular RNA (Fig. 3B). Moreover, a FISH assay revealed that Circ_0002970 was localized mostly in the cytoplasm of RA-FLSs but not in the nucleus (Fig. 3C). The presence of back-splicing was confirmed by Sanger sequencing of the RT-PCR amplification product for circ_0002970, which was identified by its expected size (Fig. 3D). Moreover, circ_0002970 was resistant to RNase R digestion (Fig. 3E).

Effects of circ_0002970 knockdown on RA-FLS migration, invasion and MMP expression

A specific small interfering RNA (siRNA) was designed to knockdown circ_0002970 expression, and the si-circ_0002970-2 with the highest knockdown efficiency

was selected (Fig. 4A). To investigate the function of circ_0002970 in RA progression, we transfected circ_0002970 siRNA into RA-FLSs to interfere with its expression. Compared with those in the si-NC control group, the invasion and migration of RA-FLSs were inhibited by circ_0002970 knockdown in transwell assays (Fig. 4B). Furthermore, the expression of MMP-9 and MMP-13 in RA-FLSs was decreased by Circ_0002970 knockdown, with no significant effect on the expression levels of MMP-1 and MMP-3 (Fig. 4C). These findings were further verified at the protein level via western blot analysis. After circ_0002970 was knocked down, the protein expression levels of MMP-9 and MMP-13 were significantly downregulated (Fig. 4E). Furthermore, the ELISA results demonstrated that IL-6 secretion in RA-FLSs was reduced by the knockdown of circ_0002970 (Fig. 4F).

Differential expression and functional enrichment analysis of genes after knockdown of circ_0002970

RNA sequencing was performed to analyze gene expression changes between the si-circ_0002970 group ($n=3$) and the NC group ($n=3$) in RA-FLSs. The distribution of differentially expressed genes (DEGs) between these two groups was visualized using box plots, heatmaps, and volcano plots (Fig. 5A-C). GO enrichment analysis showed that these DEGs were enriched in biological process (BP), molecular function (MF), and cellular component (CC) categories. In the CC category, the DEGs were significantly enriched in terms related to cytoskeleton, focal adhesion, and cell projection (Fig. 5D). In the BP category, the most significantly enriched GO terms included negative regulation of cell migration and protein dephosphorylation (Fig. 5E). In the MF category, the DEGs were primarily enriched in protein binding and kinase activity (Fig. 5F). KEGG pathway enrichment analysis revealed that the DEGs were predominantly enriched in the Hippo signaling pathway (Fig. 5G). Compared to the NC group, the mRNA levels of CCN1 and CTGF, downstream targets of the Hippo-YAP pathway, were significantly downregulated in the si-circ_0002970 group (Fig. 5H). Western blot analysis further confirmed that the key components of the Hippo-YAP pathway, including CCN1, CTGF, and YAP, were downregulated following circ_0002970 knockdown (Fig. 5I). The quantification of CCN1, CTGF, and YAP protein expression was normalized to Tubulin (Fig. 5J). These results suggest

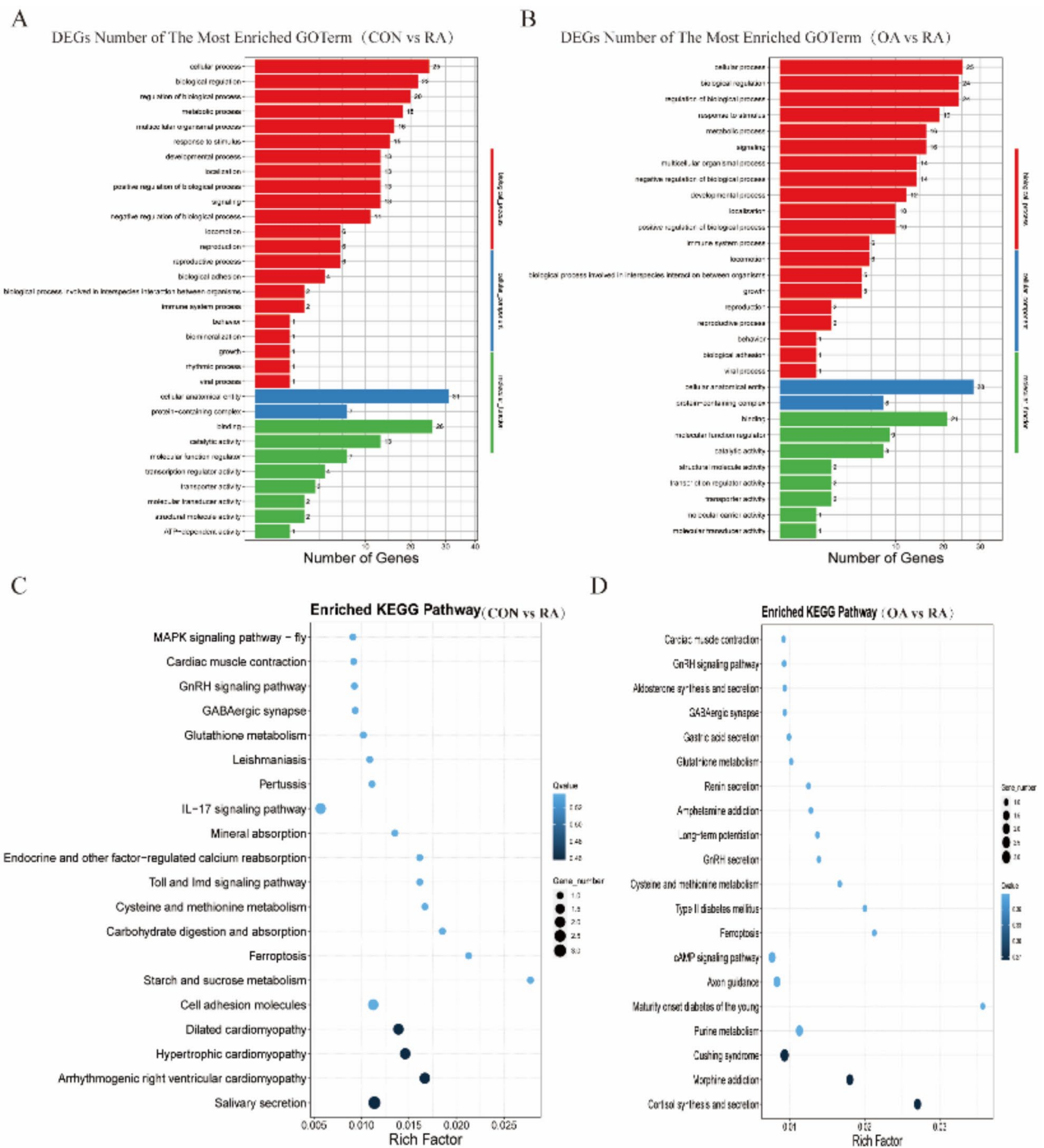


Fig. 2 GO and KEGG Pathway Enrichment Analysis of Differentially Expressed Genes. (A-B) GO term enrichment analysis of DEGs. Bar graphs display the most significantly enriched Gene Ontology (GO) terms in CON vs. RA (A) and OA vs. RA (B) comparisons. (C-D) KEGG pathway enrichment analysis of DEGs. Bubble chart illustrate significantly enriched KEGG pathways for CON vs. RA and OA vs. RA comparisons

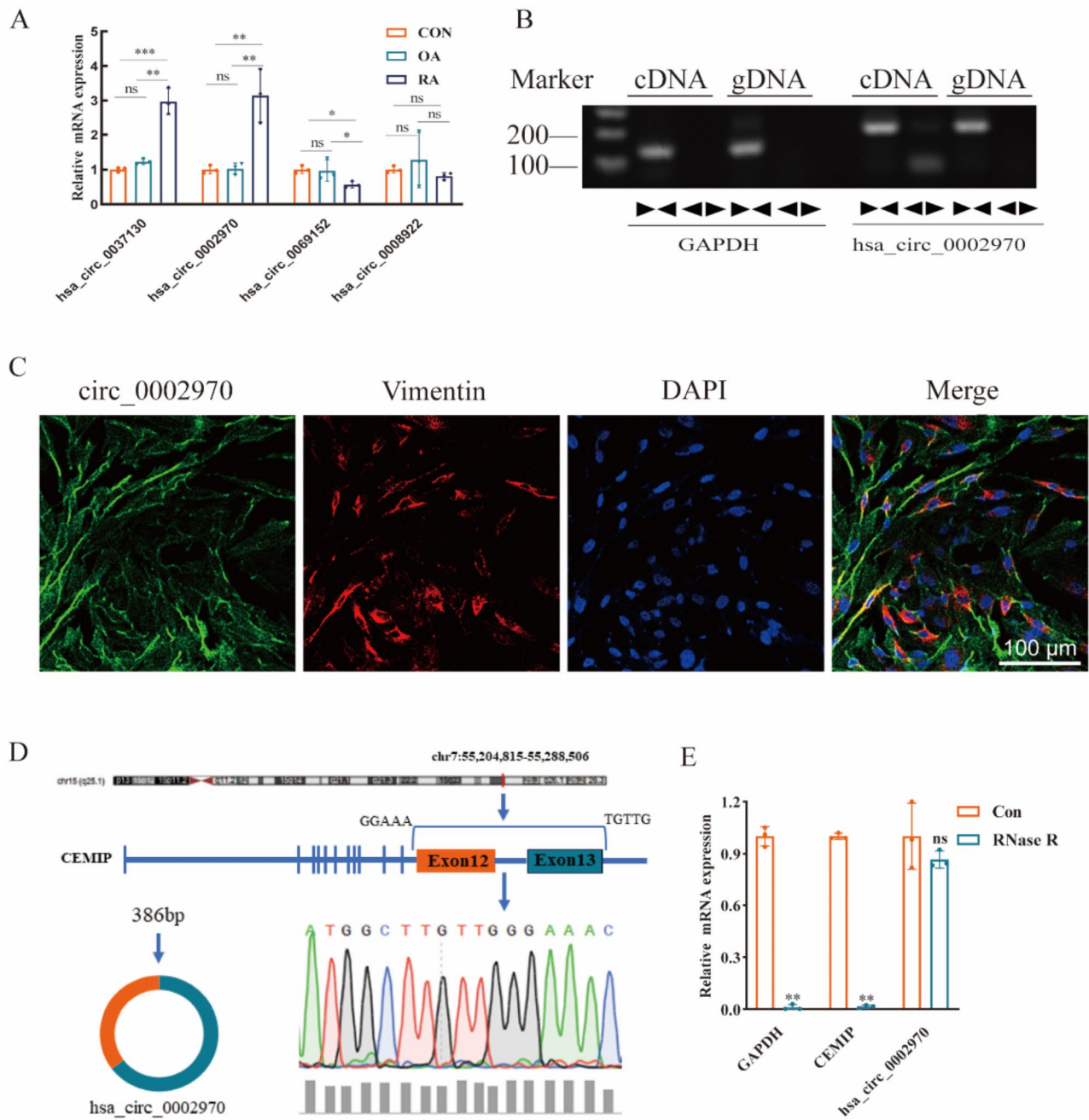


Fig. 3 Identification and Characterization of circ_0002970 in RA-FLSs. **(A)** Expression analysis of differentially expressed circRNAs in RA-FLSs. qRT-PCR results show the relative expression levels of circRNAs in RA, OA, and CON groups. **(B)** Confirmation of the circular structure of circ_0002970. Divergent primers could amplify Circ_0002970 from cDNA but not from gDNA. **(C)** Subcellular localization of circ_0002970 in RA-FLSs. RNA FISH reveals that circ_0002970 (green) colocalizes with the mesenchymal marker Vimentin (red) in the cytoplasm. **(D)** Genomic origin and back-splicing junction validation of circ_0002970. Circ_0002970 is derived from the CEMIP gene, consisting of exons 12 and 13, with Sanger sequencing confirming the back-splicing junction. **(E)** qRT-PCR results show that circ_0002970 is resistant to RNase R digestion, whereas linear RNAs (GAPDH, CEMIP) are significantly degraded. Scale bar, 100 μm. Data are shown as mean ± SD. NS, not significant. **p* < 0.05, ***p* < 0.01, ****p* < 0.001

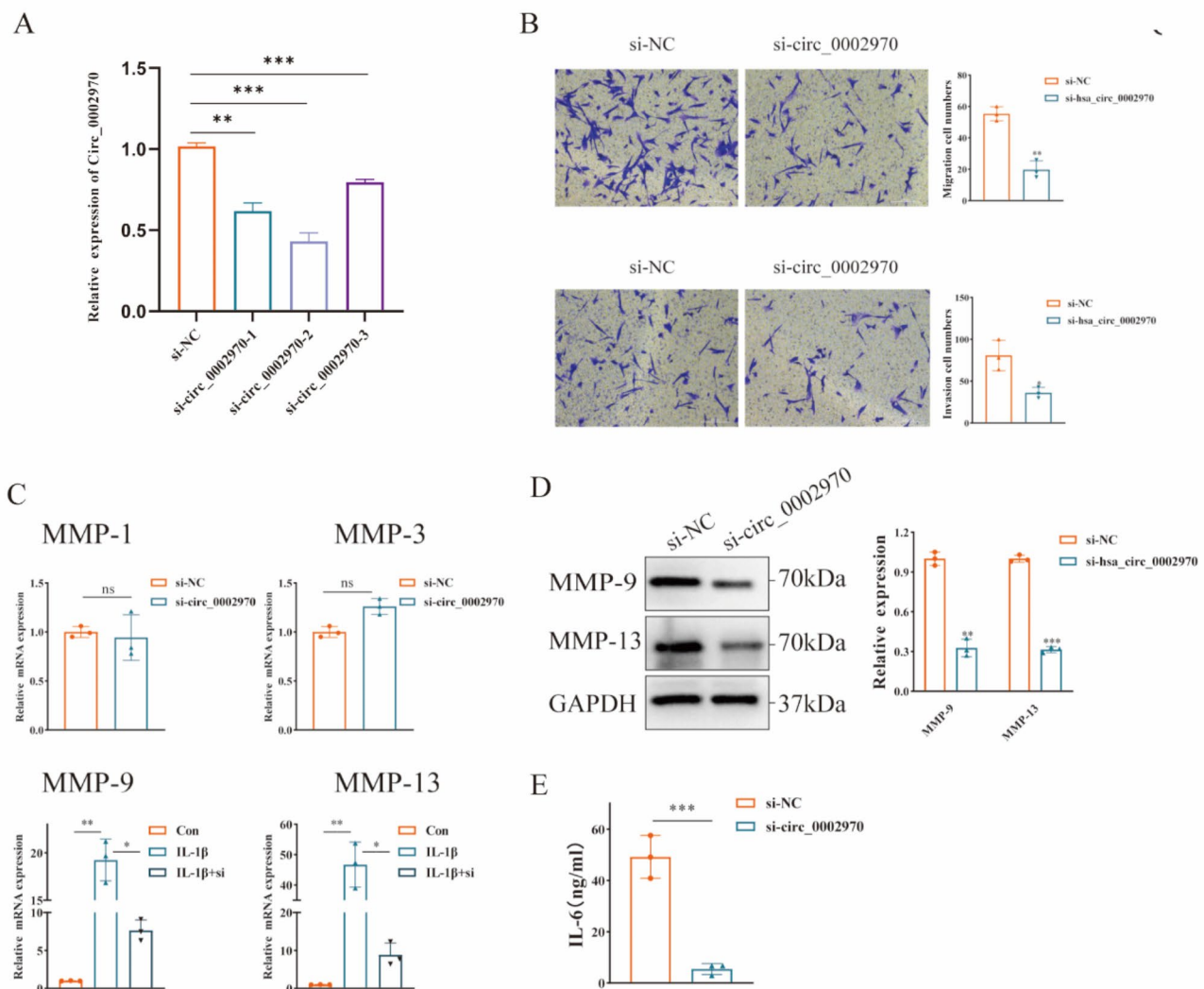


Fig. 4 Circ_0002970 Knockdown Inhibits RA-FLS Migration, Invasion, and Inflammatory Response. **(A)** Knockdown efficiency of circ_0002970. qRT-PCR confirms the significant reduction of circ_0002970 expression in RA-FLSs transfected with siRNAs. **(B)** Reduced migration and invasion after circ_0002970 knockdown. Transwell assays show decreased RA-FLS migratory and invasive capacities upon circ_0002970 silencing. **(C)** Effect on MMP expression. qRT-PCR shows that circ_0002970 knockdown significantly reduces MMP-9 and MMP-13 levels, while MMP-1 and MMP-3 remain unchanged. **(D)** Western blot validation of MMP downregulation. Circ_0002970 knockdown decreases MMP-9 and MMP-13 protein levels in RA-FLSs. **(E)** ELISA shows a significant decrease in IL-6 levels after circ_0002970 knockdown. Scale bar, 200 μ m. Data are shown as mean \pm SD. NS, not significant. * $p < 0.05$, ** $p < 0.01$, *** $p < 0.001$

that circ_0002970 regulates RA-FLS function through the Hippo-YAP signaling pathway, affecting cell migration and invasion.

Effects of circ_0002970 on RA-FLS migration and invasion through the Hippo/YAP signaling pathway

To investigate the effect of Hippo-YAP pathway activation on RA-FLS migration and invasion, we conducted rescue experiments using the Hippo-YAP inhibitor verteporfin (VP). The results revealed that in the over-expression group (OE) treated with VP, the level of YAP was significantly reduced (Fig. 6A). The results indicated that circ_0002970 significantly promoted the migration

and invasion of RA-FLSs. When the YAP pathway was inhibited, the number of migrating and invading RA-FLSs decreased (Fig. 6B-C). These results indicate that circ_0002970 may regulate the migration and invasion of RA-FLSs via the Hippo-YAP signaling pathway.

Discussion

Synovitis is the core pathological feature and a key factor controlling the progression of RA. There is increasing evidence that RA-FLSs can promote synovial hyperplasia and pannus formation and that FLSs are critical in RA pathogenesis [27]. In this study, we detected the circRNA expression profile of RA-FLSs. We found that

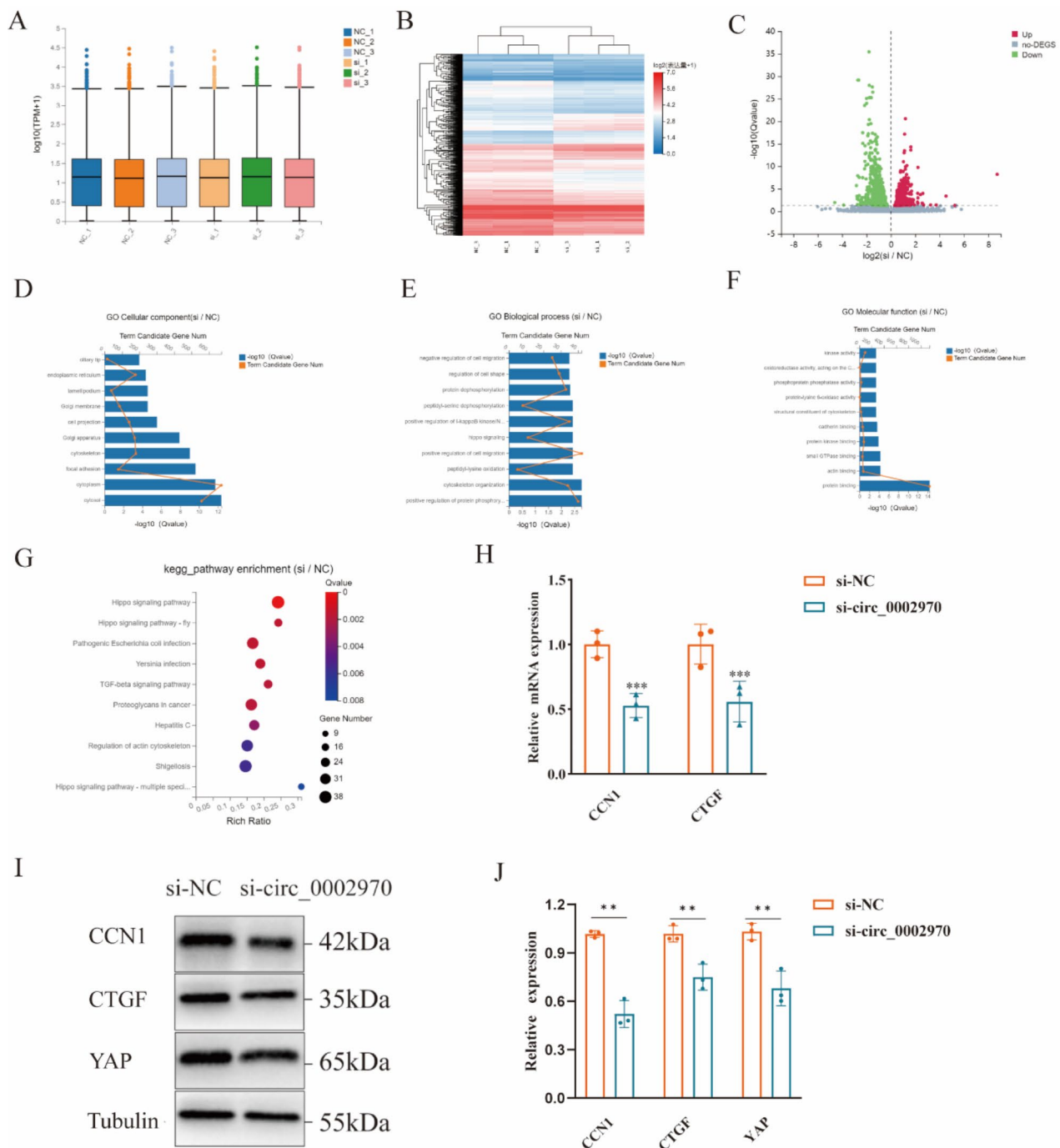


Fig. 5 Transcriptomic and Functional Effects of circ_0002970 Knockdown in RA-FLS. **(A)** Gene expression distribution. Box plot showing the $\log_{10}(\text{FPKM} + 1)$ values across si-NC and si-circ_0002970 groups. **(B)** Hierarchical clustering of DEGs. Heatmap illustrating upregulated and downregulated genes after circ_0002970 knockdown. **(C)** Volcano plot of DEGs. Upregulated and downregulated genes identified in the si-circ_0002970 group. **(D-F)** GO enrichment analysis. Enriched cellular components, biological processes, and molecular functions influenced by circ_0002970 knockdown. **(G)** KEGG pathway enrichment analysis. Bubble plot showing significantly enriched pathways. **(H)** qRT-PCR validation of CCN1 and CTGF expression. Knockdown of circ_0002970 significantly reduces CCN1 and CTGF mRNA levels compared to si-NC. **(I)** Western blot validation of Hippo-YAP pathway regulation. Circ_0002970 knockdown decreases CCN1, CTGF, and YAP1 protein levels. **(J)** Western blot quantification. CCN1, CTGF, and YAP1 protein expression normalized to Tubulin. Data are shown as mean \pm SD. ** $p < 0.01$, *** $p < 0.001$

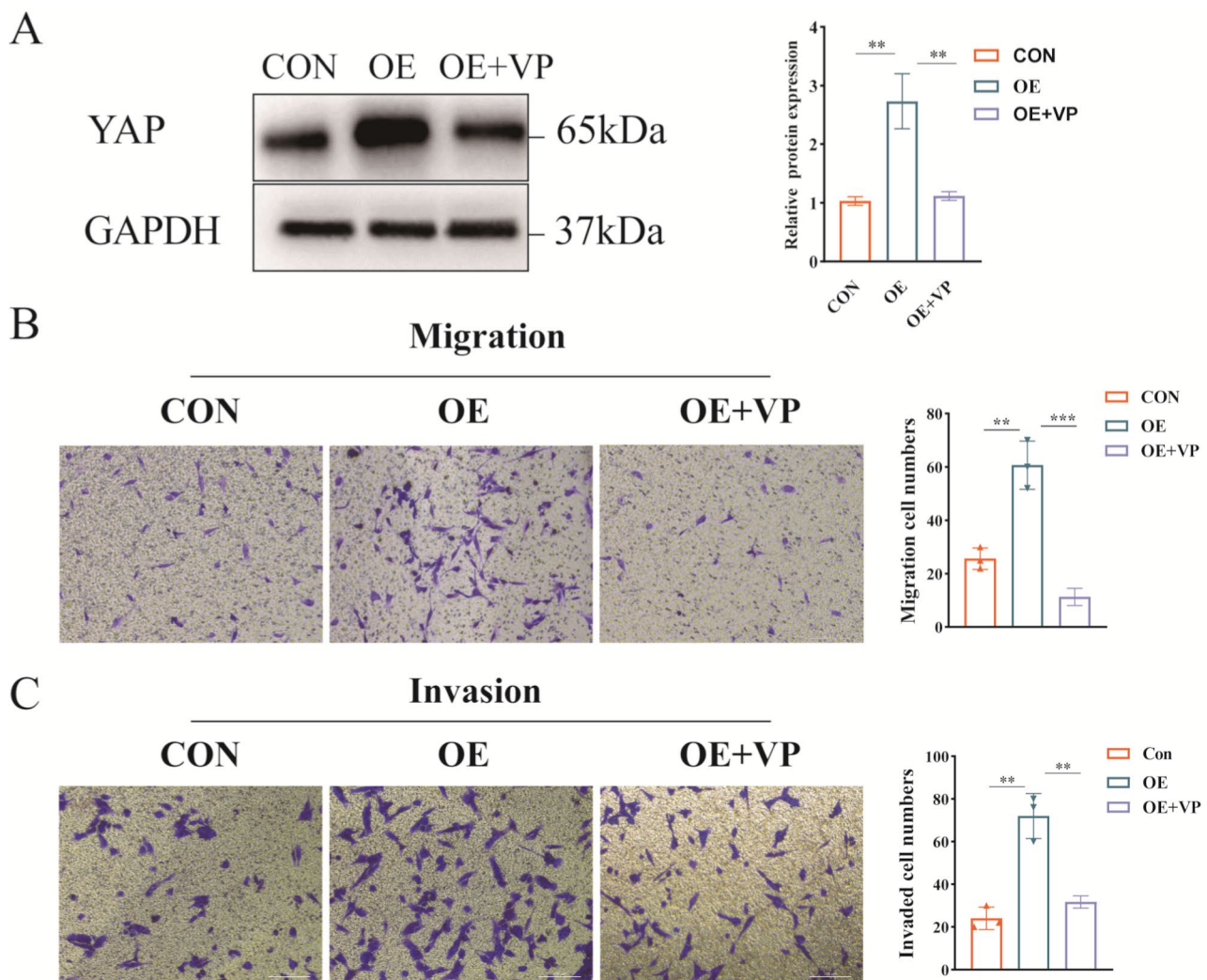


Fig. 6 Circ_0002970 Overexpression Enhances RA-FLS Migration and Invasion via the Hippo-YAP Pathway. **(A)** Western blot analysis of YAP expression. YAP protein levels increase with circ_0002970 overexpression (OE) and decrease upon verteporfin (VP) treatment. **(B-C)** Effect of circ_0002970 overexpression on RA-FLS migration and invasion. Transwell assays show that circ_0002970 overexpression significantly enhances RA-FLS migration and invasion, while VP treatment reverses these effects. Scale bar, 200 μ m. Data are shown as mean \pm SD. ** $p < 0.01$, *** $p < 0.001$

circ_0002970 was aberrantly upregulated in RA patients compared with OA patients and healthy controls. We analyzed the role of circ_0002970 knockdown in RA-FLS migration, invasion and the inflammatory response. We subsequently found that circ_0002970 could induce CTGF/CCN1 through the Hippo-YAP signaling pathway to prevent the progression of RA (FLS).

Circ_0002970 was backspliced by CEMIP mRNA exons 12–13. Many studies have shown that CEMIP expression is increased in RA-FLSs compared with that in OA patients and healthy controls [28]. Moreover, the expression of CEMIP is related to the severity of RA [29]. In our study, analogous effects of circ_0002970 in RA were also observed. Usually, circRNAs exhibit functional similarities to their host genes and are expressed asynchronously [30, 31]. CEMIP expression is increased in the FLSs of

OA patients compared with healthy controls but remains lower than that in the FLSs of RA patients [28, 32]. Previous studies have shown that the knockdown of circRNAs in RA decreases the migration and invasion of FLSs [23, 33]. In our study, we found that circ_0002970 knockdown inhibited the migration and invasion of RA-FLSs and that CEMIP expression was unaffected.

RA-FLSs can secrete inflammatory factors such as IL-6, IL-8, and IL-17. IL-8 is an essential inflammatory chemokine that activates inflammatory cells, prompting them to converge on inflammatory foci and release inflammatory mediators, thereby causing pain in RA patients [34]. Studies have shown that FLSs in the synovial lining are the primary source of IL-6, with cultured FLSs spontaneously producing IL-6, while IL-1 or TNF- α stimulation further enhances its secretion, potentially via

the NF- κ B signaling pathway [9]. IL-6 has been identified as a key driver of synovial inflammation, activating multiple signaling pathways and inducing the secretion of additional proinflammatory mediators, thereby perpetuating the inflammatory cycle [35]. By demonstrating that circ_0002970 regulates inflammatory factors, we observed a decrease in IL-6 expression following circ_0002970 knockdown, confirming its role in reducing the inflammatory response. Previous studies have shown that RA-FLSs can be stimulated by IL-1 β and TNF- α . Specifically, IL-1 β has been demonstrated to induce the transition of RA-FLSs from a quiescent state to an activated state [9]. We found that the expression of MMP-9 and MMP-13 without stimulation by inflammatory factors was relatively low. Consequently, *in vitro* stimulation with cytokines such as IL-1 β can increase MMP expression. QRT-PCR analysis revealed that the knockdown of circ_0002970 had no significant effect on MMP-1 and MMP-3 expression, indicating that circ_0002970 exerts minimal influence on these MMPs. However, we observed a significant downregulation of MMP-9 and MMP-13 following circ_0002970 knockdown, suggesting that circ_0002970 primarily regulates specific MMPs in RA-FLSs rather than broadly affecting all MMPs. The expression of different MMPs may be governed by distinct regulatory mechanisms, and circ_0002970 appears to specifically influence regulatory factors associated with MMP-9 and MMP-13. Research indicates that through degradation mediated by matrix metalloproteinases (MMP-13 or MMP-9), chondrocyte apoptosis and matrix loss occur, thereby exacerbating cartilage destruction [36, 37].

We performed transcriptome sequencing on RA-FLSs with and without circ_0002970 knockdown to identify differentially expressed genes (DEGs), followed by GO and KEGG enrichment analyses. GO analysis revealed that in the biological process (BP) category, DEGs were predominantly enriched in the positive and negative regulation of cell migration and the Hippo signaling pathway. In the molecular function (MF) and cellular component (CC) categories, the enriched terms were primarily associated with cell migration and invasion-related functions. KEGG pathway analysis further demonstrated that among the top ten enriched signaling pathways, three were closely related to the Hippo signaling pathway, highlighting its potential involvement in circ_0002970-mediated RA-FLS dysfunction.

The increased invasiveness of RA-FLSs is intricately linked to the modulation of diverse signaling pathways and their associated proteins, such as the Hippo–YAP signaling pathway. This signaling pathway modulates cellular proliferation, apoptosis, migration, and other processes, influencing cellular growth and development [38]. Prior studies have shown a notable increase in YAP

expression in patients with RA, and dysregulation of the Hippo–YAP signaling pathway can exacerbate inflammation and the severity of joint damage in patients with RA [39, 40]. The overexpression of YAP resulted in the upregulation of MMP-1 and MMP-13 secretion by IL-1 β - and TNF- α -stimulated RA-FLSs, promoting the migration and invasion capabilities of RA-FLSs [39, 41]. Our study revealed that knockdown of circ_0002970 resulted in downregulation of YAP expression, as well as downregulation of the downstream proteins CCN1 and CTGF in the Hippo–YAP signaling pathway. CCN1, as an integral part of the extracellular matrix (ECM), actively participates in various functions, including endothelial cell adhesion, migration, proliferation, and other cellular processes [42]. The cardinal functions of CTGF are associated with inflammation, fibrosis, and endochondral ossification of cartilage [43, 44]. Therefore, we speculate that circ_0002970 induces CTGF/CCN via the Hippo–YAP signaling pathway to regulate the migration, invasion, and release of inflammatory factors in RA-FLSs. This finding implies an association between circ_0002970 and RA pathogenesis, suggesting that targeting circ_0002970 may be a potential therapeutic strategy for RA.

Conclusion

Our study revealed a significant upregulation of circ_0002970 in synoviocytes derived from RA patients. Furthermore, we demonstrated that knockdown of circ_0002970 could modulate the progression of RA by affecting the Hippo–YAP signaling pathway. However, this study focused only on the relationship between circ_0002970 and the Hippo–YAP signaling pathway and failed to comprehensively consider the cross-regulation of multiple signaling pathways, which is a direction for future research. This study proposes circ_0002970 as a potential therapeutic target for future RA treatment, facilitating drug development and clinical translation in the circRNA field to broaden therapeutic options for patients.

Abbreviations

RA	Rheumatoid arthritis
FLSs	Fibroblast-like synoviocytes
OA	Osteoarthritis
MMPs	Matrix metalloproteinases
CircRNAs	Circular RNAs
HE	Hematoxylin–eosin
DEGs	Differentially expressed genes
BP	Biological processes
MF	Molecular functions
CC	Cellular components
KEGG	Kyoto Encyclopedia of Genes and Genomes
siRNA	Small interfering RNA
ECM	Extracellular matrix
VP	Verteporfin
OE	Overexpression

Supplementary Information

The online version contains supplementary material available at <https://doi.org/10.1186/s13075-025-03562-3>.

Supplementary Material 1

Acknowledgements

None.

Author contributions

HK, YQ and DQ performed the data analyses and wrote the manuscript. SZ, YL and TL helped perform the analysis with constructive discussions. ZC, JF and YL revised the manuscript. All authors read and approved the final manuscript.

Funding

This study was financially supported by the Henan Provincial Key Research and Development Program (241111313400), Henan Provincial Medical Science and Technology Research Program (232102310105) and Henan Provincial Medical Science and Technology Research Program (232102310076).

Data availability

No datasets were generated or analysed during the current study.

Declarations

Ethics approval and consent to participate

Ethical approval was obtained from the Ethics Committee of Henan Provincial People's Hospital (LLXJS2023-1-137). Informed consent forms were signed by all individuals prior to acquiring and studying their tissues.

Consent for publication

Not applicable.

Competing interests

The authors declare no competing interests.

Author details

¹Zhengzhou University People's Hospital & Henan Provincial People's Hospital, No. 7 Weiwu Road, Zhengzhou, Henan, China

Received: 20 December 2024 / Accepted: 14 April 2025

Published online: 25 April 2025

References

- Smith MH, Berman JR. What is rheumatoid Arthritis? [J]. *JAMA*. 2022;327(12):1194. <https://doi.org/10.1001/jama.2022.0786>
- McInnes IB, Schett G. The pathogenesis of rheumatoid arthritis [J]. *N Engl J Med*. 2011;365(23):2205–19. <https://doi.org/10.1056/NEJMr1004965>
- Abbasi M, Mousavi MJ, Jamalzehi S, et al. Strategies toward rheumatoid arthritis therapy; the old and the new [J]. *J Cell Physiol*. 2019;234(7):10018–31. <https://doi.org/10.1002/jcp.27860>
- Smolen JS, Breedveld FC, Burmester GR, et al. Treating rheumatoid arthritis to target: 2014 update of the recommendations of an international task force [J]. *Ann Rheum Dis*. 2016;75(1):3–15. <https://doi.org/10.1136/annrheumdis-2015-207524>
- Aletaha D, Smolen JS. Diagnosis and management of rheumatoid arthritis: A Review [J]. *JAMA*. 2018;320(13):1360–72. <https://doi.org/10.1001/jama.2018.13103>
- Calvo Alén J, Pérez T, Romero Yuste S, et al. Efficacy and safety of combined therapy with synthetic Disease-modifying antirheumatic drugs in rheumatoid arthritis: systematic literature Review [J]. *Reumatol Clin (Engl Ed)*. 2020;16(5 Pt 1):324–32. <https://doi.org/10.1016/j.reuma.2018.07.016>
- Ma JD, Jing J, Wang JW, et al. A novel function of Artesunate on inhibiting migration and invasion of fibroblast-like synoviocytes from rheumatoid arthritis patients [J]. *Arthritis Res Ther*. 2019;21(1):153. <https://doi.org/10.1186/s13075-019-1935-6>
- Karami J, Aslani S, Tahmasebi MN, et al. Epigenetics in rheumatoid arthritis; fibroblast-like synoviocytes as an emerging paradigm in the pathogenesis of the disease [J]. *Immunol Cell Biol*. 2020;98(3):171–86. <https://doi.org/10.1111/mcb.12311>
- Bartok B, Firestein GS. Fibroblast-like synoviocytes: key effector cells in rheumatoid arthritis [J]. *Immunol Rev*. 2010;233(1):233–55. <https://doi.org/10.1111/j.0105-2896.2009.00859.x>
- Sabeh F, Fox D, Weiss SJ. Membrane-type I matrix metalloproteinase-dependent regulation of rheumatoid arthritis synoviocyte function [J]. *J Immunol*. 2010;184(11):6396–406. <https://doi.org/10.4049/jimmunol.0904068>
- Laragione T, Brenner M, Li W, et al. Cia5d regulates a new fibroblast-like synoviocyte invasion-associated gene expression signature [J]. *Arthritis Res Ther*. 2008;10(4):R92 <https://doi.org/10.1186/ar2476>
- Gibbons LJ, Hyrich KL. Biologic therapy for rheumatoid arthritis: clinical efficacy and predictors of response [J]. *BioDrugs*. 2009;23(2):111–24. <https://doi.org/10.2165/00063030-200923020-00004>
- Yoshitomi H. Regulation of immune responses and chronic inflammation by Fibroblast-Like Synoviocytes [J]. *Front Immunol*. 2019;10:1395. <https://doi.org/10.3389/fimmu.2019.01395>
- Køster D, Egedal JH, Lomholt S, et al. Phenotypic and functional characterization of synovial fluid-derived fibroblast-like synoviocytes in rheumatoid arthritis [J]. *Sci Rep*. 2021;11(1):22168. <https://doi.org/10.1038/s41598-021-01692-7>
- Alunno A, Carubbi F, Giacomelli R, et al. Cytokines in the pathogenesis of rheumatoid arthritis: new players and therapeutic targets [J]. *BMC Rheumatol*. 2017;1:3 <https://doi.org/10.1186/s41927-017-0001-8>
- Müller-Ladner U, Kriegsmann J, Franklin BN, et al. Synovial fibroblasts of patients with rheumatoid arthritis attach to and invade normal human cartilage when engrafted into SCID mice [J]. *Am J Pathol*. 1996;149(5):1607–15.
- Pan YH, Wu WP, Xiong XD. Circular RNAs: promising biomarkers for Age-related Diseases [J]. *Aging Dis*. 2020;11(6):1585–93. <https://doi.org/10.14336/ajcd.2020.0309>
- Eger N, Schoppe L, Schuster S, et al. Circular RNA Splicing [J]. *Adv Exp Med Biol*. 2018;1087:41–52. https://doi.org/10.1007/978-981-13-1426-1_4
- Wang C, Liu WR, Tan S, et al. Characterization of distinct circular RNA signatures in solid tumors [J]. *Mol Cancer*. 2022;21(1):63. <https://doi.org/10.1186/s12943-022-01546-4>
- Chen I, Chen CY, Chuang TJ. Biogenesis, identification, and function of exonic circular RNAs [J]. *Wiley Interdiscip Rev RNA*. 2015;6(5):563–79. <https://doi.org/10.1002/wrna.1294>
- Memczak S, Jens M, Elefsinioti A, et al. Circular RNAs are a large class of animal RNAs with regulatory potency [J]. *Nature*. 2013;495(7441):333–8. <https://doi.org/10.1038/nature11928>
- Hansen TB, Jensen TI, Clausen BH, et al. Natural RNA circles function as efficient MicroRNA sponges [J]. *Nature*. 2013;495(7441):384–8. <https://doi.org/10.1038/nature11993>
- Cai Y, Liang R, Xiao S, et al. Circ_0088194 promotes the invasion and migration of rheumatoid arthritis Fibroblast-Like synoviocytes via the miR-766-3p/MMP2 Axis [J]. *Front Immunol*. 2021;12:628654 <https://doi.org/10.3389/fimmu.2021.628654>
- Harvey KF, Pflieger CM, Hariharan IK. The Drosophila Mst ortholog, Hippo, restricts growth and cell proliferation and promotes apoptosis [J]. *Cell*. 2003;114(4):457–67. [https://doi.org/10.1016/s0092-8674\(03\)00557-9](https://doi.org/10.1016/s0092-8674(03)00557-9)
- Zhou W, Shen Q, Wang H et al. Knockdown of YAP/TAZ Inhibits the Migration and Invasion of Fibroblast Synovial Cells in Rheumatoid Arthritis by Regulating Autophagy [J]. *J Immunol Res*. 2020;2020:9510594. <https://doi.org/10.1155/2020/9510594>
- Arnett FC, Edworthy SM, Bloch DA, et al. The American rheumatism association 1987 revised criteria for the classification of rheumatoid arthritis [J]. *Arthritis Rheum*. 1988;31(3):315–24. <https://doi.org/10.1002/art.1780310302>
- Mor A, Abramson SB, Pillingner MH. The fibroblast-like synovial cell in rheumatoid arthritis: a key player in inflammation and joint destruction [J]. *Clin Immunol*. 2005;115(2):118–28. <https://doi.org/10.1016/j.clim.2004.12.009>
- Yoshida H, Nagaoka A, Kusaka-Kikushima A, et al. KIAA1199, a deafness gene of unknown function, is a new hyaluronan binding protein involved in hyaluronan depolymerization [J]. *Proc Natl Acad Sci U S A*. 2013;110(14):5612–7. <https://doi.org/10.1073/pnas.1215432110>
- Zhang W, Yin G, Zhao H, et al. Secreted KIAA1199 promotes the progression of rheumatoid arthritis by mediating hyaluronic acid degradation in an ANXA1-dependent manner [J]. *Cell Death Dis*. 2021;12(1):102. <https://doi.org/10.1038/s41419-021-03393-5>

30. Salzman J, Chen RE, Olsen MN, et al. Cell-type specific features of circular RNA expression[J]. *PLoS Genet.* 2013;9(9):e1003777. <https://doi.org/10.1371/journal.pgen.1003777>
31. Zhang Y, Xue W, Li X, et al. The biogenesis of nascent circular RNAs[J]. *Cell Rep.* 2016;15(3):611–24. <https://doi.org/10.1016/j.celrep.2016.03.058>
32. Deroyer C, Charlier E, Neuville S, et al. CEMIP (KIAA1199) induces a fibrosis-like process in Osteoarthritic chondrocytes[J]. *Cell Death Dis.* 2019;10(2):103. <http://doi.org/10.1038/s41419-019-1377-8>
33. Zhao P, Ma G, Ma L. Circ_0000479 promotes proliferation, invasion, migration and inflammation and inhibits apoptosis of rheumatoid arthritis fibroblast-like synoviocytes via miR-766/FKBP5 axis[J]. *J Orthop Surg Res.* 2023;18(1):220. <https://doi.org/10.1186/s13018-023-03700-0>
34. He R, Li X, Zhang S, et al. Dexamethasone inhibits IL-8 via Glycolysis and mitochondria-related pathway to regulate inflammatory pain[J]. *BMC Anesthesiol.* 2023;23(1):317. <https://doi.org/10.1186/s12871-023-02277-9>
35. Avci AB, Feist E, Burmester GR. Targeting IL-6 or IL-6 receptor in rheumatoid arthritis: what have we Learned?[J]. *BioDrugs.* 2024;38(1):61–71. <https://doi.org/10.1007/s40259-023-00634-1>
36. Dayer JM, De Rochemonteix B, Burrus B, et al. Human Recombinant Interleukin 1 stimulates collagenase and prostaglandin E2 production by human synovial cells[J]. *J Clin Invest.* 1986;77(2):645–8. <https://doi.org/10.1172/jci112350>
37. Kovács B, Vajda E, Nagy EE. Regulatory effects and interactions of the Wnt and OPG-RANKL-RANK signaling at the Bone-Cartilage interface in Osteoarthritis[J]. *Int J Mol Sci.* 2019;20(18). <https://doi.org/10.3390/ijms20184653>
38. Kong H, Han JJ, Gorbachev D, et al. Role of the Hippo pathway in autoimmune diseases[J]. *Exp Gerontol.* 2024;185:112336. <https://doi.org/10.1016/j.exger.2023.112336>
39. Caire R, Audoux E, Courbon G, et al. YAP/TAZ: key players for rheumatoid arthritis severity by driving fibroblast like synoviocytes phenotype and Fibro-Inflammatory Response[J]. *Front Immunol.* 2021;12:791907. <https://doi.org/10.3389/fimmu.2021.791907>
40. Wang T, Wang Z, Qi W, et al. Possible future avenues for rheumatoid arthritis therapeutics: Hippo Pathway[J]. *J Inflamm Res.* 2023;16:1283–96. <https://doi.org/10.2147/jir.S403925>
41. Symons RA, Colella F, Collins FL, et al. Targeting the IL-6-Yap-Snail signalling axis in synovial fibroblasts ameliorates inflammatory arthritis[J]. *Ann Rheum Dis.* 2022;81(2):214–24. <https://doi.org/10.1136/annrheumdis-2021-220875>
42. Lau LF. CCN1/CYR61: the very model of a modern matricellular protein[J]. *Cell Mol Life Sci.* 2011;68(19):3149–63. <https://doi.org/10.1007/s00018-011-0778-3>
43. Perbal B. CCN proteins: multifunctional signalling regulators[J]. *Lancet.* 2004;363(9402):62–4. [https://doi.org/10.1016/s0140-6736\(03\)15172-0](https://doi.org/10.1016/s0140-6736(03)15172-0)
44. Takigawa M, Nakanishi T, Kubota S, et al. Role of CTGF/HCS24/ecogenin in skeletal growth control[J]. *J Cell Physiol.* 2003;194(3):256–66. <https://doi.org/10.1002/jcp.10206>

Publisher's note

Springer Nature remains neutral with regard to jurisdictional claims in published maps and institutional affiliations.